

Oblique Plate Convergence, Slip Vectors, and Forearc Deformation

ROBERT MCCAFFREY

Department of Earth and Environmental Sciences, Rensselaer Polytechnic Institute, Troy, New York

Slip vectors from thrust earthquakes at subduction zones where convergence is oblique to the trench often point between the directions of relative plate convergence and normal to the trench axis, suggesting that oblique convergence is taken up by partial decoupling. Decoupling means that a component of arc-parallel motion of the leading edge of the upper plate results in less oblique thrusting at the trench. Partial decoupling is modeled by partitioning of oblique convergence into slip on thrust and strike-slip faults that are parallel to the trench and to each other and, starting with a force equilibrium condition, a relationship between the obliquity and the earthquake slip vector orientation is derived. Assuming that either fault slips when shear stress on it reaches a yield stress, oblique slip parallel to the plate vector should occur on the thrust fault when obliquity is smaller than a critical angle. For obliquity at or greater than this angle the stress on the strike-slip fault is large enough to start it slipping, and when both faults are active, the arc-parallel motion of the forearc deflects the slip vector back toward the trench-normal. If we assume that continued slip on either fault occurs at constant stress (but the two faults can be at different stresses), the slip vector will maintain a constant angle relative to the trench-normal even when obliquity is larger than the critical angle. This limiting angle of the slip vector, called Ψ_{\max} (measured relative to the trench-normal), is simply the arcsine of the ratio of the shear forces resisting slip on the strike-slip and thrust faults. A consequence is that when the obliquity exceeds Ψ_{\max} , the slip vectors on the thrust fault are sensitive only to the thrust fault orientation and contain no information about the convergence direction between the plates. Slip vectors at the Java trench southwest of Sumatra show the relationship clearly with $\Psi_{\max}=20^{\circ}\pm 5^{\circ}$, while slip vectors at the Aleutian trench show the relationship less clearly with $\Psi_{\max}=25^{\circ}$ to 45° . The greater angle at the Aleutian trench suggests that the upper plate is stronger in the Aleutian arc (relative to the thrust fault) than in the Sumatran arc, consistent with the Sumatran arc being continental and having a well-developed strike-slip fault while the Aleutian arc is oceanic and without a clear transcurrent fault. Slip vectors at the Philippine trench which, like Sumatra, has a large strike-slip fault inboard of it, tend to stay within 25° of the trench-normal when obliquity is as large as 50° . If obliquity exceeds Ψ_{\max} and continues to increase along a subduction zone, the rate of motion of the forearc relative to the upper plate will vary with obliquity, in which case the forearc sliver should extend or contract parallel to the arc. From the geometry of modern island arcs, arc-parallel extension should be the more common and has been hypothesized for both Sumatra and the Aleutians on the basis of earthquake slip vectors and for these and other arcs from geological observations. From estimates of Ψ_{\max} and the arc-parallel gradients in obliquity, arc-parallel strain rates are estimated to be 1 to 3×10^{-8} /yr for the Sumatran forearc, 2 to 6×10^{-8} /yr for the Aleutian forearc, and 0.3 to 3×10^{-8} /yr for the Philippine forearc. Oblique convergence and subsequent arc-parallel extension, if accompanied by crustal thinning, may provide an important yet little appreciated mechanism for bringing high-grade metamorphic rocks to the surface of subduction complexes.

INTRODUCTION

Fitch [1972] presented evidence for decoupling of oblique plate convergence into a component of convergence normal to the plate boundary and a shear component taken up by strike-slip faulting on a transcurrent fault within the overriding plate. He presented a few examples of where this occurs, but clearly the best is Sumatra [see Jarrard, 1986]. Fitch and then later workers [e.g., Beck, 1983, 1986; Michael, 1990; Walcott, 1978] analyzed decoupling by considering only the end-member cases of either oblique slip, where subduction slip vector azimuths remain parallel to the plate convergence vector, or complete decoupling, where deformation of the forearc takes up all of the arc-parallel component of relative plate motion so that thrusting is perpendicular to the strike of the thrust fault. While decoupling appears to be nearly complete in some continental plate boundaries [Abers and McCaffrey, 1988; McKenzie and Jackson, 1983; Molnar, 1988; Mount and Suppe, 1987], in many oceanic

subduction zones, earthquake slip vectors are neither normal to the trench nor parallel to the relative plate convergence direction, suggesting that there is a configuration between oblique slip and complete decoupling that oblique subduction systems follow. The goal of this paper is to present a simple analysis based on force equilibrium that can explain this observation and elucidate the physical parameters that control it. I also consider the effects of changes in convergence obliquity along a margin and the response of forearcs to the arc-parallel horizontal gradients in arc-parallel horizontal shear stress that arise.

Figures 1 and 2 summarize the evidence that partially decoupled slip occurs at the Sumatran, Aleutian, and Philippine subduction zones. Figure 1 shows that slip vectors from subduction thrust earthquakes align neither with the trench-normals, which would indicate complete decoupling, nor with the orientations of plate convergence, which would indicate oblique slip without deformation of the upper plate. It could be argued fairly that the trend of the trench axis is not a good indicator of the strike of the thrust plane beneath the forearc so that the appearance of oblique slip is due to error in the estimate of the trench strike. Figure 2 addresses this possibility by demonstrating that along the Sumatran and Aleutian arcs the rake angles are significantly different from 90° and therefore that there is a significant strike-

Copyright 1992 by the American Geophysical Union.

Paper number 92JB00483.
0148-0227/92/92JB-00483\$05.00

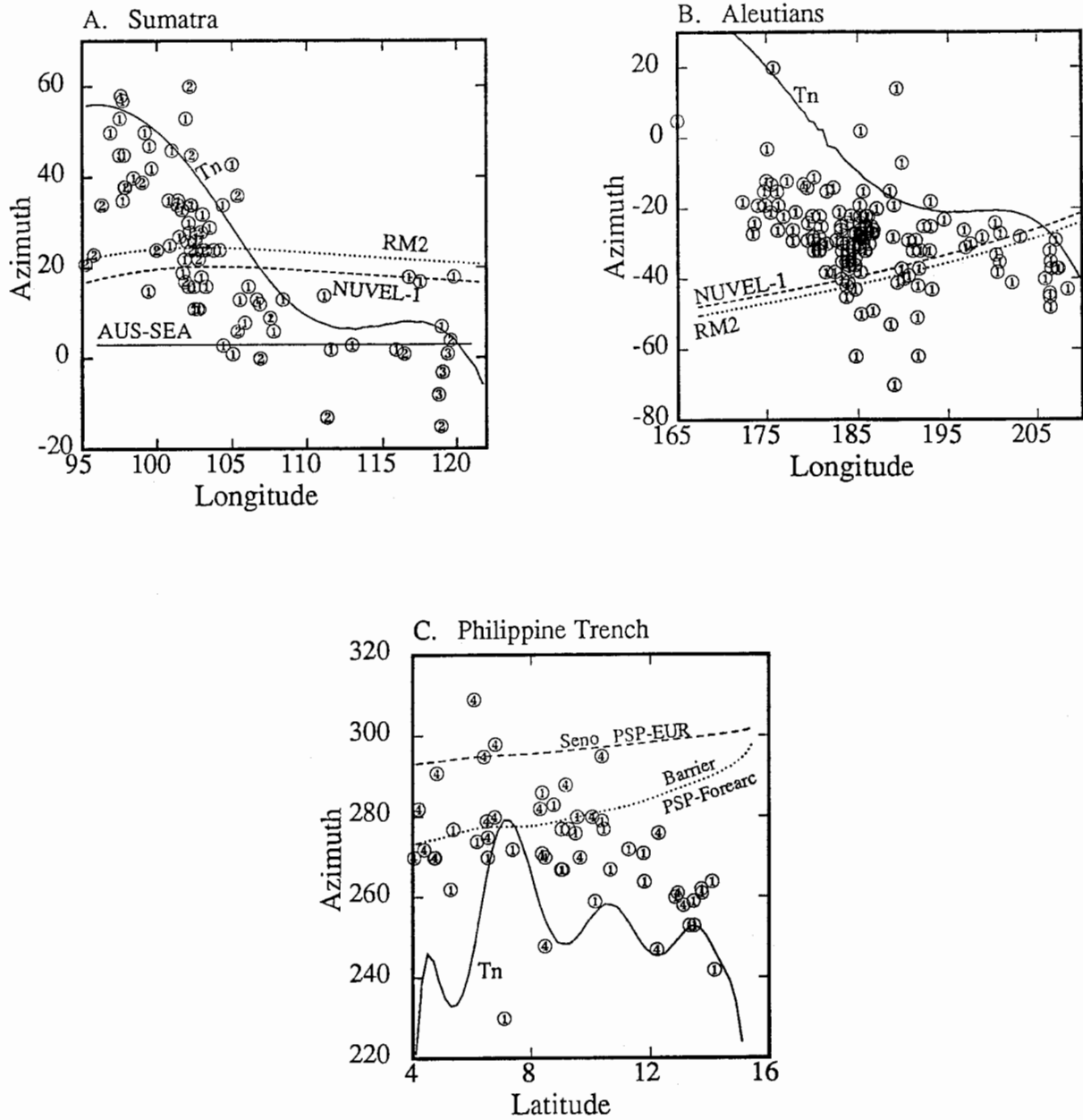


Fig. 1. Slip vector azimuths for thrust earthquakes at the Java, Aleutian, and Philippine trenches; those labeled (1) are centroid-moment tensor (CMT) solutions from *Dziewonski et al.* [1981], (2) are first-motion solutions compiled by *Kappel* [1980], (3) are body waveform solutions by *McCaffrey* [1988] and (4) are first-motion solutions compiled by *Barrier et al.* [1991]. The fault planes are assumed to be the more gently, arcward dipping planes, and the slip vector is the pole of the auxiliary plane. The azimuth of the slip vector is the angle it makes relative to north found by rotating the slip vector about the strike into the horizontal plane. Because the auxiliary planes are very steep for these earthquakes, the slip vector tends to be constrained very well by first-motion and body waveform solutions (uncertainties of $\pm 15^\circ$ in trend and $\pm 5^\circ$ in plunge for the slip vector from an individual earthquake are typical). Comparisons of the CMT solutions to body waveform solutions suggest that they have similar uncertainties [*McCaffrey*, 1988] and that the effects of the subducted slab on the solutions are small [*Ekström and Engdahl*, 1989; *McCaffrey*, 1988]. Sumatran and Aleutian trench outlines were estimated from digital bathymetry (DBDB5 that provides an average depth about every 9 km) by taking the point of maximum depth that is closest to the island arcs and smoothing. The normal to this curve was taken as the trench-normal (labeled Tn). The Philippine trench outline was taken from *Barrier et al.* [1991]. The curves labeled RM2 [*Minster and Jordan*, 1978] and NUVEL-1 [*DeMets et al.*, 1990] show plate convergence directions from Euler poles for (a) Australia-Eurasia and for (b) Pacific-North America. (a) The curve labeled AUS-SEA is the convergence direction used for Australia-Southeast Asia, inferred from slip vectors at the Java trench east of 110°E [*McCaffrey*, 1991]. (c) The predicted direction for Philippine-Eurasia (labeled PSP-EUR) is from the pole of *Seno et al.* [1987], and the dotted line is the predicted direction of thrusting of the Philippine Sea plate relative to the forearc, from the pole of *Barrier et al.* [1991].

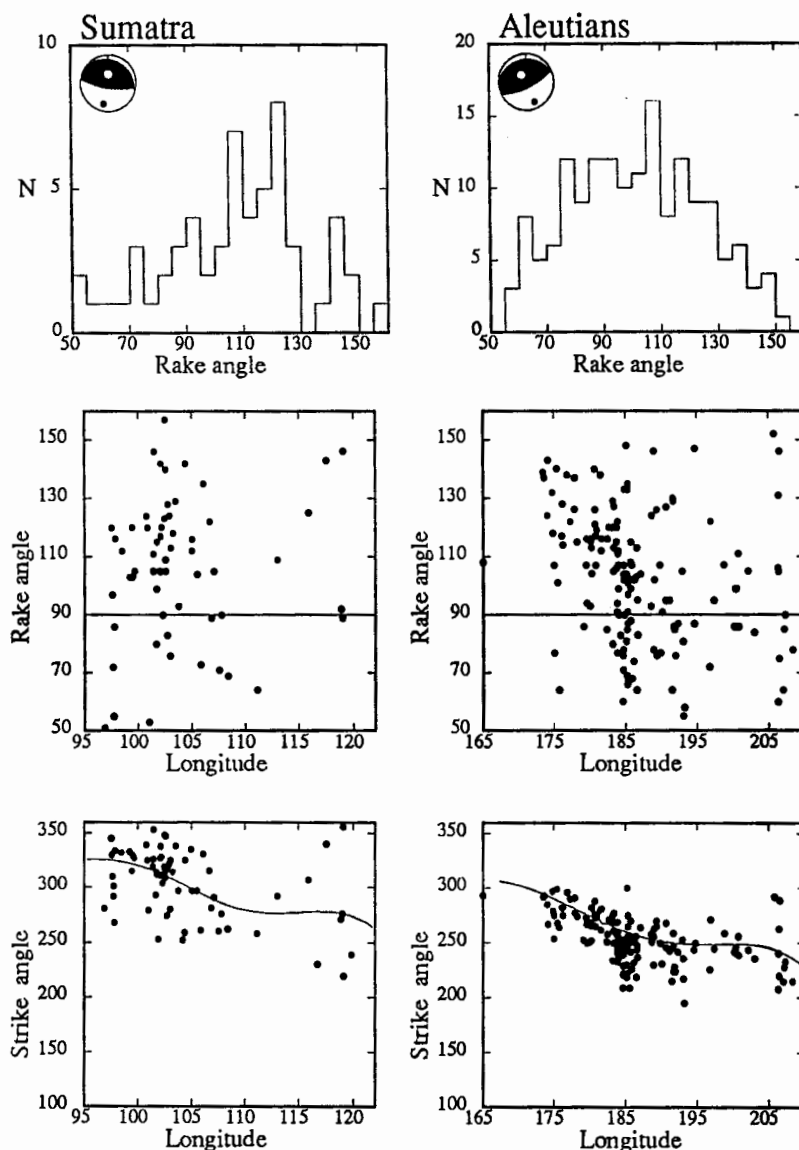


Fig. 2. Evidence that thrust earthquakes along the Sumatran and Aleutian oblique subduction zones show oblique slip (i.e., the rake angle is not 90°). Histograms of rake angles show clear shifts in both cases towards angles greater than 90° , indicating a component of right-lateral slip. This shift is evidence, independent of knowing the trench azimuth, that oblique slip occurs. The middle plots show how the rake angles vary along the margins. The bottom plots show that the strikes of the earthquakes' fault planes generally are parallel to the trends of the trenches (solid lines) and therefore that the trench trends are unbiased indicators of the strike of the subduction zone faults. Only CMT solutions are used in these plots for the following reason. The beachballs in the top plots show typical mechanisms for earthquakes on the trenches in that the fault planes are parallel to the average orientations of the thrust planes and the rake angles are the means of the observed rake angles (rake = 110° for Sumatran and 105° for the Aleutians). If these solutions were constrained with P-wave first motions, the rake angle would certainly be set to 90° , and we would miss the point. The CMT solutions are unlikely to be biased in this respect.

slip component in the centroid-moment tensor solutions of thrust earthquakes. Both are systematically shifted toward having a right-lateral component of slip. Figure 2 also shows that the trench outline is generally parallel to the strikes of the earthquake fault planes.

ANALYSIS OF OBLIQUE CONVERGENCE

Beck [1991] and McCaffrey [1990] expanded earlier analyses [e.g., Beck, 1983, 1986; Fitch, 1972; Michael, 1990; Walcott, 1978] of decoupling by allowing the slip direction between the

subducting plate and the forearc (the slip vector) to vary between the end-member cases of pure decoupling and pure oblique slip. All of these derivations were based on finding the configuration that resulted in the least amount of energy dissipation per unit convergence. Here, I generalize partial decoupling by allowing the slip vector to vary between the directions perpendicular to the trench and parallel to the plate convergence direction and solve the problem starting with a force-balance condition. The force-balance and minimum energy dissipation approaches give the same result with the appropriate assumptions, although I suggest that Beck's [1991] minimum energy solution be amended to account for an

error in his expression for the slip vector. I see two reasons for doing the problem with force-balance rather than minimum energy dissipation constraints; first, not everyone believes that minimizing energy dissipation is as fundamental physics as the balance of forces [e.g., *Bird and Yuen, 1979*] and, having done the problem initially with energy minimization [*McCaffrey, 1990*], I find that the physical insight gained is much greater when one considers forces instead of energy.

In the block model (Figure 3), the velocity vector of the subducting plate (Plate 1) relative to the upper plate (Plate 2) has a magnitude v and makes an angle γ (the obliquity) in the horizontal plane relative to the trench-normal (AP). The relative motion is decoupled in that slip can occur on arc-parallel strike-slip (transcurrent) and thrust (subduction) faults. These faults isolate a third block of lithosphere, called the sliver plate. I assume (1) that the motions of the blocks are resisted only on the two bounding faults (i.e., the three plates are rigid) and that the faults will slip when stress on them reaches a maximum yield stress; (2) that the problem is two-dimensional so that there is no variation in stress in the x direction (parallel to strike); (3) that forces are in equilibrium (excluding during earthquakes when accelerations occur); (4) that no body forces act in the x direction; and (5) that the stresses considered are vertically integrated. Unlike *Beck [1991]*, I allow the vertical extents of the thrust and strike-slip faults to differ.

With these assumptions, that include those implied in minimum energy arguments [*Beck, 1991*], I first show that the horizontal shear forces per unit length on the two faults are equal. Consider the structure shown in Figure 3. Shear stress resists motion from the surface to depth Z_t on the thrust fault and to Z_s on the strike-slip fault. In the Cartesian coordinate system with x parallel to the trench, y perpendicular to it, and z down, the net forces in the x direction are assumed to be zero (i.e., there are no accelerations),

$$\frac{\partial \tau_{xx}}{\partial x} + \frac{\partial \tau_{yx}}{\partial y} + \frac{\partial \tau_{zx}}{\partial z} + f_x = 0 \quad (1)$$

where f is the body force. The assumption of two dimensions

removes gradients of stress in x (i.e., $\partial \tau_{xx} / \partial x = 0$) and without body forces in the x direction, (1) becomes

$$\frac{\partial \tau_{yx}}{\partial y} + \frac{\partial \tau_{zx}}{\partial z} = 0 \quad (2)$$

The bottom of the block is at depth Z , where Z is any depth below the deeper of Z_t and Z_s . In the model the shear stress is zero between Z_t (or Z_s) and Z so the contribution to the total shear force on the fault in this depth increment is zero. Therefore, we can consider an integral of stress from the surface to depth Z as equivalent to an integral from the surface to Z_t (or Z_s). This is important because it permits the thrust and strike-slip faults to extend to different depths (as they most certainly do) while maintaining the validity of the solution. The integral (2) over depth from Z to 0 is

$$\int_0^z \frac{\partial \tau_{yx}}{\partial y} dz + \int_0^z \frac{\partial \tau_{zx}}{\partial z} dz = 0$$

and integrating the second term gives $\tau_{zx}(z=Z) - \tau_{zx}(z=0)$. At the surface $\tau_{zx} = 0$, and I assume that $\tau_{zx} = 0$ at $z=Z$ also so that this term drops out; in other words, I assume that no horizontal shear stress acts on the base of the block and Z_t and Z_s are defined as such. Therefore

$$\int_0^z \frac{\partial \tau_{yx}}{\partial y} dz = 0 \quad (3)$$

If τ'_{yx} is the vertically averaged stress τ_{yx} (from the surface to Z) then (3) indicates that $\partial \tau'_{yx} / \partial y = 0$; hence τ'_{yx} does not vary in the y direction. The vertically averaged horizontal component of shear stress on a fault striking in the x direction and dipping at an angle δ is $\tau'_{yx} \sin \delta + \tau'_{zx} \cos \delta$ where τ'_{zx} is the vertically averaged stress τ_{zx} . Because I assume that $\tau_{zx} = 0$, the horizontal shear

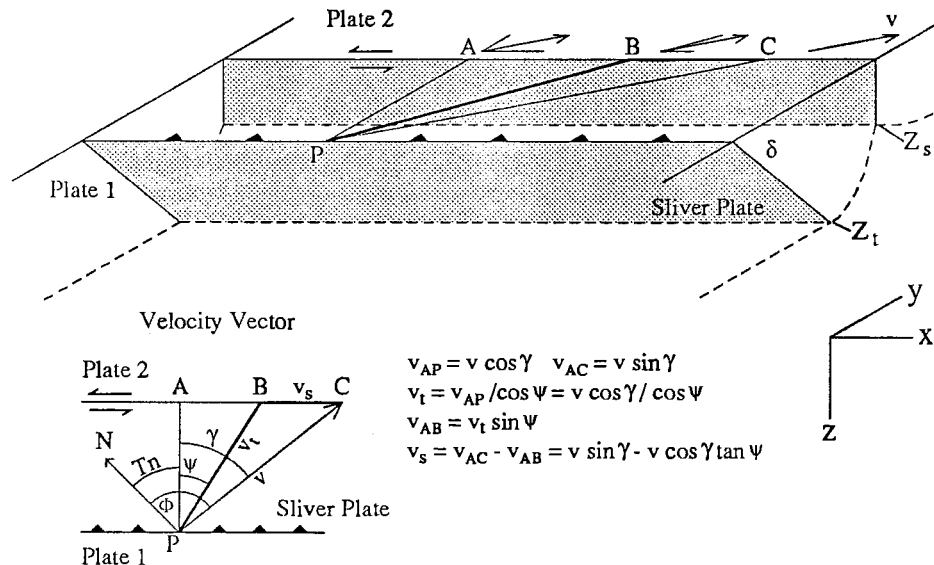


Fig. 3. Block diagram showing the geometry of thrust (with barbs) and vertical strike-slip faults. Convergence occurs in the direction of PC with a slip rate v . This slip is decoupled into thrusting of an amount v_t and strike-slip of an amount v_s . The angle γ is the obliquity (the angle between the plate convergence direction and the direction normal to the trench) while ψ is the angle the slip vector (parallel to PB) makes with the direction normal to the trench (AP). T_n is the direction of the normal to the trench (relative to north) and ϕ is the plate convergence direction. Z_t and Z_s are the vertical extents of shear stress on the thrust and strike-slip faults, respectively. The dashed line at the base of the structure shows the depths below which shear stress is assumed to be zero.

force on this plane, that extends to depth Z and has an area per unit length of $Z / \sin \delta$, is $\tau'_{yx}Z$, which is also the horizontal shear force on a vertical plane parallel to x and extending to depth Z . Hence the horizontal shear force per unit length will be the same on any plane striking parallel to x . For the reasons given above, this statement holds true even for faults that extend to different depths, as drawn in Figure 3.

The total horizontal shear force per unit length required to produce slip on the vertical strike-slip fault is $F_s = Z_s \tau'_s$, where τ'_s is the vertically averaged shear stress on the fault when it slips. The force that drives the slip on the strike-slip fault derives from the horizontal component of shear on the thrust fault. The shear force per unit length on the thrust fault needed to make it slip is $F_t = Z_t \tau'_t / \sin \delta$, where δ is the dip of the thrust fault and the subscript t refers to the thrust fault.

Next we need to characterize the slip direction on the thrust fault. Using as a reference frame the rigid part of the upper plate far from the plate boundary and the coordinate system described earlier, the motion of Plate 1 (i.e., plate convergence) is described by the vector in the horizontal plane $\mathbf{v} = v(\sin \gamma, \cos \gamma, 0)$, where γ is the angle of obliquity (Figure 3). I define the footwall vector \mathbf{f} to describe the motion of the footwall block and the hanging wall vector \mathbf{h} to describe the motion of the hanging wall of the thrust, both in the rigid upper plate reference frame; $\mathbf{f}-\mathbf{h}$ is the slip vector \mathbf{s} , which represents the motion of the footwall relative to the hanging wall. To get \mathbf{f} , \mathbf{v} is rotated about the trench axis (the x axis) through the dip angle δ to get

$$\mathbf{f} = v(\sin \gamma, \cos \gamma \cos \delta, \cos \gamma \sin \delta).$$

For a subduction zone in which the forearc is not deforming, $\mathbf{h}=0$ and \mathbf{f} is also the slip vector, whose magnitude is v .

This differs from the footwall vector used by Beck [1991], which is

$$\mathbf{f} = vA(\sin \gamma, \cos \gamma, \cos \gamma \sin \delta),$$

where the factor $A = (1 + \cos^2 \gamma \sin^2 \delta)^{-1/2}$ is needed to keep the magnitude of \mathbf{f} equal to v . I suggest that this is incorrect for the following reason. Prior to subduction the arc-parallel component of the velocity vector is $v_x = v \sin \gamma$, and after subduction, according to Beck's derivation, this component is

$$f_x = v A \sin \gamma.$$

Crossing the trench, the change in the x -component ($f_x - v_x$) is then $v(A-1) \sin \gamma$, which is zero only if $\gamma=0$. Hence, the footwall vector used by Beck implies that the subducting plate is sheared parallel to the trench axis during subduction. If one instead rotates \mathbf{v} about the horizontal trench axis to get \mathbf{f} , then the x component is $v \sin \gamma$ both before and after subduction, and no horizontal shear is required.

In expressing the slip vector in the general form $\mathbf{s}=\mathbf{f}-\mathbf{h}$, we can see that the analysis here holds for subduction zones (where we assume that $\mathbf{h}=0$), oblique fold-and-thrust belts, and transpressional strike-slip faults such as the San Andreas (where \mathbf{h} is not necessarily zero). For the latter two cases, that are the same, uplift of the hanging wall of the thrust may apparently change the slip vector \mathbf{s} . Recalling that \mathbf{f} and \mathbf{h} are in a rigid upper plate reference frame, uplift of the hanging wall produces a nonzero \mathbf{h} by rotation (a translation is simply a rotation about a very distant axis). For the two-dimensional problem, uplift of the hanging wall is a rotation about a horizontal axis parallel to the x axis. If we say that the fault plane is attached to the hanging wall then the fault plane experiences the same rotation as \mathbf{h} . The expression for the slip vector is then $\mathbf{s} = \mathbf{f} - \mathbf{h}\mathbf{R}$, where \mathbf{R} is the rotation matrix operating on the hanging wall. Multiplying through by the inverse of \mathbf{R} , we get $\mathbf{s}\mathbf{R}^{-1} = \mathbf{f}\mathbf{R}^{-1} - \mathbf{h}$, which is applying the inverse rotation to \mathbf{f} , \mathbf{s} , and the fault plane. Rotation of \mathbf{h} will result in rotation of \mathbf{s} but will also cause the same rotation of the

fault plane; therefore, most importantly, \mathbf{s} does not change in the frame of the fault plane.

The important point of the foregoing discussion for our purposes is that the trench-parallel (x) component of the footwall vector (per unit convergence) does not change after subduction and so is given by $\sin \gamma$. The horizontal component of shear force on the thrust fault parallel to x is

$$F_x = Z_t \tau'_t \sin \gamma / \sin \delta.$$

For small values of γ such that $F_x < F_s$, where F_s was defined earlier as the force required to move the strike-slip fault, shear stress on the strike-slip fault is not large enough to make it slip, and pure oblique slip will occur on the thrust fault. In this range of γ , the slip vector azimuth should be parallel to the plate convergence vector so $\Psi=\gamma$, and we can write

$$F_x = Z_t \tau'_t \sin \psi / \sin \delta.$$

At another point along the arc (or perhaps at some later time), a larger γ produces a larger F_x and at some point γ may reach a critical angle at which F_x equals F_s . At this point Ψ still equals γ but the strike-slip fault will be activated because its yield stress has been reached. Motion on the strike-slip fault causes Ψ to deviate from γ . If the stress on the strike-slip fault cannot exceed this yield stress (i.e., no strain hardening), then the angle Ψ cannot increase beyond this critical angle, whereas γ can. Therefore Ψ reaches a maximum, called Ψ_{\max} , when $F_x=F_s$ and the strike-slip fault is active. Where γ is greater than Ψ_{\max} , as traction grows on the thrust fault, the strike-slip fault will slip first and slip such an amount that the slip vector is deflected back toward the trench normal until it makes an angle Ψ_{\max} with the trench-normal. If $\gamma > \Psi_{\max}$, then the forearc sliver moves parallel to the arc (in the x direction) relative to the reference frame (Figure 3) and

$$\mathbf{h} = v(\sin \gamma - \cos \gamma \tan \Psi_{\max}, 0, 0).$$

In this case the slip vector is

$$\mathbf{s} = \mathbf{f}-\mathbf{h} = v(\cos \gamma \tan \Psi_{\max}, \cos \gamma \cos \delta, \cos \gamma \sin \delta),$$

which has a length of $v \cos \gamma / \cos \Psi_{\max}$. It can be shown using the dot product that the slip vector \mathbf{s} makes an angle Ψ_{\max} relative to the unit trench normal vector \mathbf{T}_n in the plane of the thrust fault, where $\mathbf{T}_n = (0, \cos \delta, \sin \delta)$.

As γ increases (spatially or temporally), the strike-slip fault first slips at a point where $\gamma=\Psi_{\max}$, so by equating the horizontal shear forces on the two faults at that point, we can write

$$Z_s \tau'_s = Z_t \tau'_t \sin \Psi_{\max} / \sin \delta \quad (4)$$

or

$$R_f = \sin \Psi_{\max} = Z_s \tau'_s \sin \delta / Z_t \tau'_t \quad (5)$$

where R_f is simply the ratio of the shear forces resisting motion on the two active faults. The results above are the same as those derived by minimizing frictional energy dissipated by the two faults [McCaffrey, 1990] but differ from those of Beck [1991] because of the difference in the calculation of the slip vector, as noted above, and because I do not assume that $Z_s=Z_t$.

An important consequence of the foregoing analysis is that at points along the margin where γ exceeds Ψ_{\max} , the earthquake slip vector azimuths will remain at angle Ψ_{\max} relative to the trench normal and are therefore independent of the plate convergence vector. Kinematically, the additional component of relative plate motion parallel to the trench due to γ exceeding Ψ_{\max} will increase the slip rate on the strike-slip fault; this motion on the strike-slip fault deflects the slip vectors on the thrust fault back to Ψ_{\max} . When $\gamma > \Psi_{\max}$, the slip vector should vary only with the

orientation of the thrust fault, so that in the plots of Figure 1, at large obliquity the slip vectors and the trench-normal curves should be approximately parallel and the angle between them is simply Ψ_{\max} . This independence of Ψ_{\max} and γ allows us to estimate Ψ_{\max} from the slip vectors and trench orientation without detailed knowledge of the plate convergence vector.

Arc-Parallel Strain Rates

The independence of γ and Ψ_{\max} (when $\gamma > \Psi_{\max}$) also has important implications for the kinematics of oblique convergence. The deviations of slip vectors from expected azimuths in both Sumatra and the Aleutians have been cited as evidence for arc-parallel stretching of the forearcs [Ekström and Engdahl, 1989; McCaffrey, 1991]. Avé Lallemant and Guth [1990] presented a geometrical argument for why forearc slivers stretch when obliquity increases due to a bend in the subduction trench. They presented a simple analog by pushing cardboard beneath a table with a curved edge and used disks for the forearc blocks. The disks could rotate only about a horizontal axis parallel to the table top, so their analog was for the case of complete decoupling. Arc-parallel deformation of the sliver plate results from a gradient in the angle of obliquity that produces an arc-parallel gradient in the horizontal shear stress on the upper plate. This force produces permanent strain in the forearc wherever the angle of obliquity exceeds Ψ_{\max} (this is merely a statement of the kinematics because it is time-dependent strain in the forearc that allows Ψ to deviate from γ). Here I derive the relevant expressions.

The time-averaged slip rate of the forearc sliver relative to the upper plate is given by

$$v_s = v (\sin \gamma - \cos \gamma \tan \Psi) \quad (6)$$

where Ψ is used here in the general sense as shown in Figure 3. Where $\gamma = \Psi$, $v_s = 0$; where $\gamma > \Psi$, $v_s > 0$; and if $\gamma - \Psi$ increases with increasing γ , v_s will also increase with γ . This is a kinematic constraint and does not depend on assumptions of the mechanical behavior of the forearc. Therefore, if the prediction that Ψ reaches a maximum value is correct (that does depend on rheology assumed), then for $\gamma > \Psi_{\max}$, the slip rate of the forearc relative to the upper plate should increase with increasing obliquity γ , resulting in an arc-parallel deformation rate gradient within the forearc. If obliquity did not vary along the margin, then the forearc block could move rigidly. Most modern island arcs display a large trench-parallel gradient in the obliquity (Figure 4).

The sense of the deformation (i.e., arc-parallel stretching or shrinking) depends on the geometry of the margin and the variation in slip direction. In the case of a margin that is convex toward the subducting plate (Figure 5a) or where the change in obliquity is such that the relative plate motion vectors diverge (Figure 5b), the forearc should stretch. If the margin is concave toward the ocean (Figure 5c) or the relative plate motion vectors converge (Figure 5d), the forearc should shrink parallel to the arc. For the cases of Sumatra [McCaffrey, 1991] and the Aleutians [Ekström and Engdahl, 1989], the margin is convex toward the oceanic subducting plate so that the increase in the angle of obliquity causes the plate convergence vectors to diverge, and extension is expected. Most island arcs are convex toward the subducting plate side, as in Figure 5a, so it is likely that arc-parallel extension will be the more common.

The strain rate can be predicted if Ψ_{\max} and the arc-parallel variation in obliquity ($d\gamma/dx$) are known. For sections of the forearc where $\gamma > \Psi_{\max}$, the arc-parallel gradient in v_s is

$$\begin{aligned} \frac{dv_s}{dx} = v \frac{d\gamma}{dx} (\cos \gamma + \tan \Psi_{\max} \sin \gamma) \\ + \frac{dv}{dx} (\sin \gamma - \tan \Psi_{\max} \cos \gamma) \end{aligned} \quad (7)$$

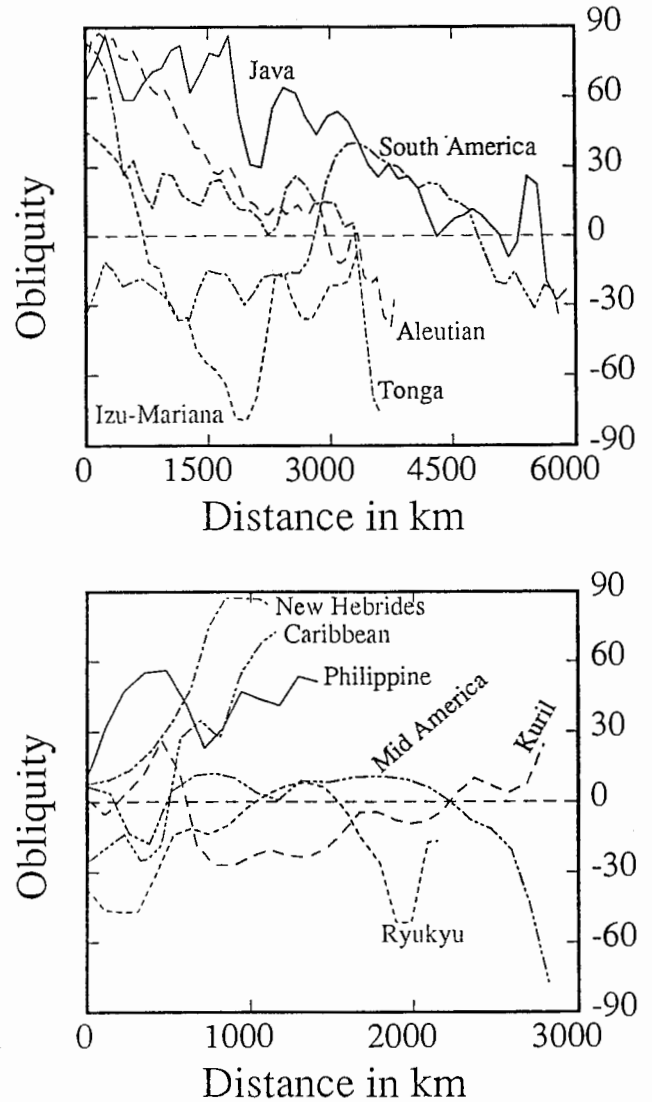


Fig. 4. Variation of obliquity along many of the world's trenches. Distances are measured along the trench. Plate vectors are taken from DeMets *et al.* [1990] and Seno *et al.* [1987], and trench outlines were determined as described in Figure 1.

where the x axis is locally parallel to the arc. The first term on the right side is commonly much larger than the second term, so the strain rate estimate is roughly proportional to the plate velocity and the gradient in the obliquity. Hence the estimate of strain rate is not very sensitive to uncertainties in the location of the pole of rotation if the pole is far from the plate boundary. This expression can be shown to hold for curved arcs by letting $dx = r d\theta$, where r is the radius of curvature for a circular trench segment and $d\theta$ is the infinitesimal angle subtended at the center of curvature by that segment of trench.

Estimating the Ratio of Shear Stress on the Two Faults

Several workers have used the expressions of Beck [1983, 1986, 1991] to estimate what Beck calls R , (τ'_s / τ'_t) the ratio of shear stresses acting on the faults. I suggest that this approach provides a useful estimate of the ratio of stresses only when Ψ_{\max} can be estimated, Z_t and Z_s are known, and obliquity is constant along the convergent margin of interest. First, the physics (force-balance or minimum energy) indicates that it is more fundamentally the ratio of the shear forces (that I call R_f), than shear stresses, on the two faults that controls the behavior of the

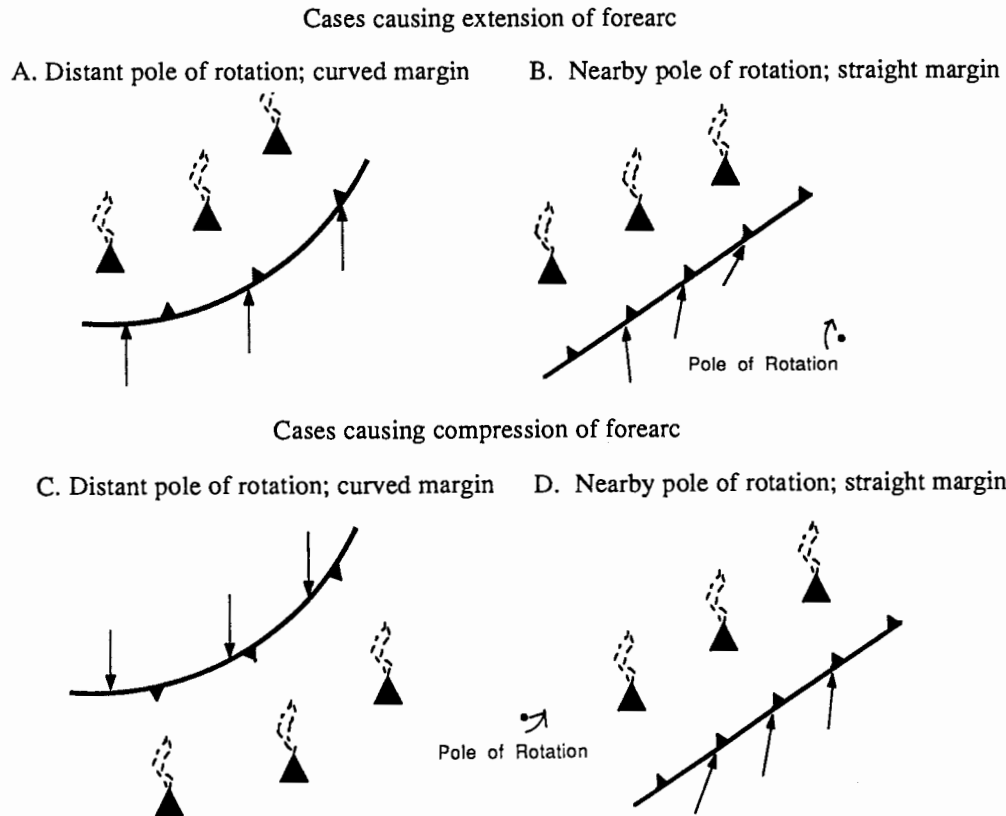


Fig. 5. Examples of convergent geometries in which obliquity may vary along the margin either by having a curved margin or a nearby pole of relative rotation between the converging plates.

slip vector ((4) and (5)). We can estimate R_f from slip vector data by constraining Ψ_{\max} . To get the ratio of stresses, one must then estimate either Z_s , Z_t , and δ or Z_s and the downdip length of the thrust fault (i.e., $Z_t/\sin \delta$). The dip angle δ can be estimated fairly well from earthquake hypocenters and fault plane solutions. Beck's derivations set Z_s equal to Z_t so these depth extents do not appear in his final equations; thus applications of his approach have not considered the vertical extents of the faults. What are the Z terms and how well do we know them? Z is the vertical extent of resistance to slip on the fault. There are few things in geology that we know less about than the depth to which fault slip is resisted [e.g., Scholz, 1990]. Maximum earthquake depths provide a bound but may in fact only include the weakest part of the fault if they do not extend into the upper mantle. Maximum depths of thrust earthquakes at subduction zones around the world vary by a factor of 2 [Sykes *et al.*, 1991] but we do not know how much deeper the resistance extends. In some cases Z_s and Z_t may be constrained by geometry, such as when the thrust fault and the strike-slip fault are known to intersect at a known depth (C. Jones, personal communication, 1991). In most cases we will realistically have to assign very large uncertainties to the vertical extents of the faults, and the estimate of R will be greatly uncertain.

A second problem arises when obliquity is not constant along strike of the margin, in which case the forearc must respond in some way to the trench-parallel gradient in shear stress at the thrust fault. Minimum energy calculations have not taken into account the work needed to deform the forearc. Only at $\gamma \geq \Psi_{\max}$ does the yield stress on the strike-slip fault come into play. However, at $\gamma > \Psi_{\max}$ (in the presence of a gradient in obliquity) the forearc is deforming in other ways than just on a single strike-slip fault and (5) no longer holds strictly. In reality, the force that we attribute to resistance on the strike-slip fault, is likely the sum of forces that resist deformation of the forearc and that resist slip on the strike-slip fault. Therefore, R in this case represents the

ratio of stress resisting deformation of the forearc to that on the thrust fault (and again only if we know Z_t and Z_s with small uncertainty).

APPLICATION TO SLIP VECTORS AT OBLIQUE CONVERGENT MARGINS

The foregoing suggests that the angle ψ between the slip vector and the trench normal should coincide with the obliquity γ when γ is small and then hold at a constant (maximum) value Ψ_{\max} for larger γ . Here I test the expected relation and estimate Ψ_{\max} at the Sumatran and Aleutian arcs, along both of which the obliquity varies by more than 60° (Figures 1 and 4). Slip vectors at the Philippine trench do not allow a strong test of the relationship because of the large variation in the orientation of the trench (Figure 1c) and the great uncertainty in the actual direction of convergence, but do show the expected behavior.

A prediction of the analysis is that at large obliquity the slip vectors should be more sensitive to the trench-normal (used as an indicator of the strike of the thrust fault) than they are to the plate convergence; this is evident in Figure 1 in that as the plate vector and trench-normal diverge (i.e., obliquity increases), the slip vectors tend to follow the trench-normal rather than the plate vector. Sumatra is the clearest example (Figure 1a), in that as obliquity increases to the west (relative to the Australia-Southeast Asia convergence direction), the slip vector azimuths follow the trench-normal and stay just below it. In the Aleutians (Figure 1b) the slip vectors appear to increase to the west of 185°E in the same sense as the trench-normal, rather than decreasing in azimuth as the plate vector does. Similarly, for the Philippine trench (Figure 1c), the slip vector azimuths appear to decrease north of 8°N following the trench-normal rather than the Philippine Sea - Eurasia plate vector. Here the slip vectors south of 10°N are consistent with the forearc being a separate, rigid plate (the dotted

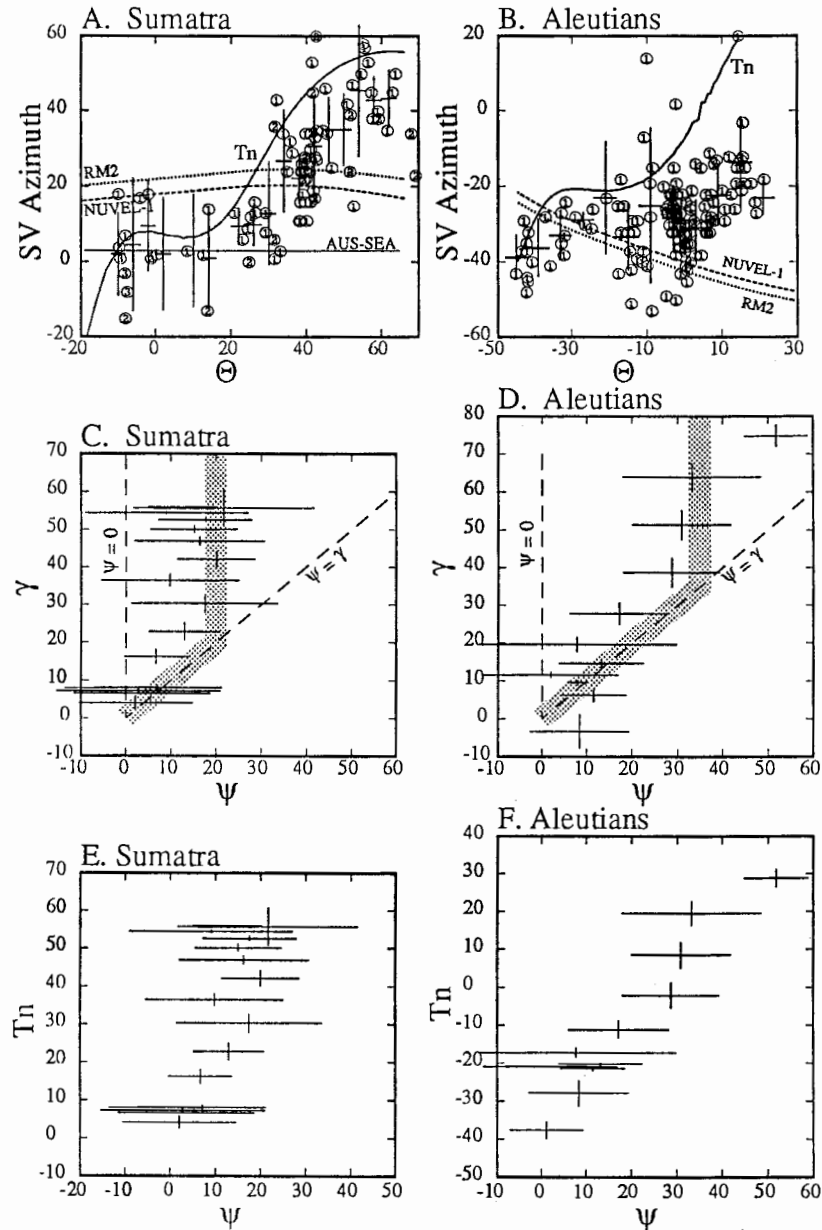


Fig. 6. (a and b) Plots of the slip vector azimuths versus the angle θ for Sumatra and the Aleutians. Angle θ is the azimuth from the point on the margin to the point forming the center of curvature of the arcs; it is used as a measure of distance along the margins for the purpose of binning the slip vector azimuths, obliquity, and trench normals to produce Figures 6c and 6d. The bars show the standard deviations of groups of slip vectors within bins of θ ; the bins are 4° (180 km) wide for Sumatra and 6° (180 km) wide for the Aleutians. Other symbols are explained in Figure 1. (c and d) Plots of Ψ (the angle the slip vector azimuth makes with the trench normal) versus the obliquity (the angle the plate convergence makes with the trench normal) for Sumatra and the Aleutians. At Sumatra the plate convergence is taken as N3°E (Australia relative to Southeast Asia). The bars reflect variations of 1 standard deviation in the obliquity, the trench normal direction and the slip vector azimuths in Figures 6a and 6b. The dashed lines show the predictions for complete decoupling ($\Psi=0$) and for oblique convergence ($\Psi=\gamma$). The theory predicts that the data points should follow the $\Psi=\gamma$ line for small values of obliquity and then reach a constant value of Ψ for large angles of obliquity. For Sumatra, the data seem to follow the expected pattern, in that they reach a constant value of $\Psi_{\max} \approx 15^\circ$ to 25° for values of obliquity of 40° to 60° . The Aleutians show the relationship less clearly with $\Psi_{\max} = 25^\circ$ to 45° (the point at $\gamma=75^\circ$ is based on only three slip vectors and may not be reliable; see Figure 4b). (e and f) Plots of Ψ versus the trench-normal azimuth, showing that Ψ_{\max} can be estimated without knowledge of the plate convergence vector.

line in Figure 1c) but north of 10°N the slip vectors clearly are strongly influenced by the trench-normal and a rigid forearc cannot match them [Barrier *et al.*, 1991].

Sumatra

Australia-Southeast Asia plate motion near Sumatra. The motion between the major plates (Australia and Southeast Asia) is

not well-known, and this will be addressed first. The motion between Australia and Eurasia is predicted by global plate motion solutions [Minster and Jordan, 1978; DeMets *et al.*, 1990]. However, Sumatra is on the Southeast Asian plate, whose motion relative to Eurasia and Australia is poorly constrained. Slip vectors south of Java (east of 105°E; Figure 1a) indicate that the motion of Australia relative to Southeast Asia is roughly north, in discord

with published Australia-Eurasia poles of rotation. Arguments can be made based on the deformation in Eurasia that Southeast Asia rotates counterclockwise relative to Eurasia so that Sumatra's longitudinal motion relative to Eurasia is eastward [McCaffrey, 1991]. This would deflect the slip vectors at the Java trench counterclockwise, i.e., in the opposite sense than they are actually deflected.

Based on the slip vectors south of Java, I infer that the motion of Australia relative to Southeast Asia is N3°E all along the margin from Java to SW Sumatra [McCaffrey, 1991]. Accordingly, obliquity at the trench increases from 0° near 110°E to about 55° at 97°E (Figures 1a and 6a). The slip vector azimuths are binned in sections along the trench (Figure 6a) so that the variations with distance along the arc are represented statistically. In the plot of observed values of Ψ versus γ (Figure 6c), the data should coincide with the line labeled $\Psi=\gamma$ where there is no decoupling and with the line labeled $\Psi=0$ for complete decoupling. For a constant value of R_f along the arc, theory predicts that the observations should fall along the $\Psi=\gamma$ line for small γ and then reach a constant value Ψ_{\max} for larger γ . The data agree with the theory in that the values of Ψ are at a nearly constant value (15°-25°) at obliquities of >30°. The angle Ψ_{\max} can also be estimated independently of the plate convergence vector (Figure 6e) as long as one is sure that the obliquity exceeds Ψ_{\max} somewhere along the trench.

Estimate of shear stress ratio for Sumatra. Here I estimate the ratio of the shear stresses acting on the two faults in Sumatra as an example of how poorly this number is constrained. The ratio R_f of the shear forces per unit length on the transcurrent fault and the subduction fault (5) ranges from 0.26 to 0.42 for $\Psi_{\max}=20^\circ\pm 5^\circ$ (Figures 6c and 6e). The shear force per unit length is the product of the vertically averaged shear stress on the fault and its downdip length so that recovery of the ratio of the shear stresses on the two faults requires estimating the downdip extent of both faults. Strike-slip earthquakes on the Sumatran fault are less than 15 km deep [Zwick and McCaffrey, 1991] but we can guess that the strength of the strike-slip fault may be significant to a depth of 60 km ($S_s=15$ to 60 km). Earthquakes on the thrust plane extend to about 60 km depth and resistance may extend to 100 km depth. The dip angle δ is $18^\circ\pm 5^\circ$, estimated from the plunges of the slip vectors, so that $S_t=(60$ to 100 km)/ $\sin(18^\circ\pm 5^\circ) \approx 150$ to 440 km. The actual length of the plate interface from the trench down to 100 km depth based on hypocenters beneath Sumatra is approximately 300 km, so this is used as an upper limit for S_t . Multiplying R_f by S_t/S_s (range of 2.5 to 20) yields a ratio of the vertically averaged shear stresses on the two faults that ranges from 0.6 to 8.4. The great range in this ratio and the fact that it brackets unity render this estimate of R of little use.

Aleutians

Obliquity along the Aleutian arc increases from 0° at about 200°E to about 60° at 175°E (Figures 1b and 6b). In contrast to Sumatra, the slip vectors appear to fall about halfway between the trench-normal curve and the plate convergence curves. Figure 6d shows that significant decoupling does not occur for γ less than 20° to 40°. In the range of $\gamma>30^\circ$, Ψ does not increase as rapidly as γ , and it is not clear whether or not Ψ reaches a constant value (even ignoring the point at $\gamma=75^\circ$, which is based on only three slip vectors). Therefore, if the hypothesis is correct, the value of Ψ_{\max} for the Aleutians must be 30° or greater, which implies that the ratio R_f for the Aleutians is greater than it is for Sumatra. This is a reasonable result, as it suggests that the forearc of the Aleutians west of 180°E, where decoupled slip is predicted to occur, is stronger than the Sumatran forearc, where a large strike-slip fault is known to exist. This inference of course presumes similarity in the thrust faults. If one accepts that the stress on a thrust fault is related to the maximum earthquake size and that we can accurately estimate the seismic moment of such large earthquakes, then the Sumatran and the Aleutian thrust zones are similar; the largest known earthquakes at the two trenches are $M_w=8.7$ for Sumatra [Newcomb and McCann, 1987] and $M_w=9.1$

for the Aleutians [Kanamori, 1978], and the dip for the Aleutian subduction zone ($21^\circ\pm 8^\circ$; the average plunge of slip vectors) is nearly the same as that for Sumatra.

ESTIMATES OF ARC-PARALLEL STRAIN RATES

Using (7), estimates of Ψ_{\max} and the gradients in obliquity along trenches, we can predict the expected strain rates of the forearcs parallel to the trench. Note that (7) includes a dependence on the obliquity γ , so the strain rate will not be constant along the forearc. Because $\gamma>\Psi_{\max}$ in the regions that undergo time dependent strain, (7) shows that the arc-parallel strain rate will decrease with increasing obliquity.

Sumatra

For Sumatra, $\Psi_{\max}=20^\circ\pm 5^\circ$, $d\gamma/dx=0.0207\pm 0.0031$ deg/km (change in obliquity of 58° along 2800 km length of the trench between 6°N, 92°E and 10°S, 110°E), and v is held constant at 70 mm/yr (i.e., $dv/dx=0$). These numbers with their uncertainties predict an arc-parallel strain rate of 2 to 3 $\times 10^{-8}$ /yr southwest of southern Sumatra where $\gamma=40^\circ$, and 1 to 2 $\times 10^{-8}$ /yr southwest of northern Sumatra, where $\gamma=70^\circ$. The slip rate of the forearc relative to Southeast Asia (6) may increase by as much as 45 to 60 mm/yr along the margin [McCaffrey, 1991]. Sieh et al. [1991] have documented slip rates on the Sumatran fault at two points separated by 320 km with a difference of 13 ± 3 mm/yr, giving a strain rate of $4.1\pm 0.9 \times 10^{-8}$ /yr.

Philippine Trench

We can estimate Ψ_{\max} at $25^\circ\pm 5^\circ$ for the Philippine trench by noting that north of 8°N where obliquity (relative to the PSP-EUR convergence direction) increases from about 40° to 55°, the slip vectors remain 20° to 30° more clockwise than the trench-normal (Figure 1c). Between 1°N and 14°N, $d\gamma/dx$ is 0.0124 ± 0.0082 deg/km, and v changes from 91 mm/yr at 1°N to 78 mm/yr at 14°N (≈ 1400 km) using the Philippine Sea - Eurasia pole of Seno et al. [1987]. Plugging these numbers into (7) gives strain rates of 1 to 3 $\times 10^{-8}$ /yr at 8°N and 0.3 to 3 $\times 10^{-8}$ /yr at 14°N. The large uncertainties derive from the large variation in the trench orientation. From 8° to 14°N the distance is 800 km, and the change in slip rate of the forearc relative to Eurasia is then 2 to 24 mm/yr for the range of estimated strain rates. The upper bound on the estimate is consistent with a kinematic analysis of slip vectors as follows. At 14°N, the Philippine Sea plate is predicted to move in the azimuth 289° at 55 mm/yr with respect to the forearc block, according to the pole of rotation estimated by Barrier et al. [1991] that fits the slip vectors south of 10°N (Figure 1c). At 14°N, slip vectors show that the motion of the Philippine Sea plate relative to the northern part of the forearc is at an azimuth of about 260°. Assuming that the northern part of the forearc moves relative to the southern forearc in a direction parallel to the trench (azimuth of 340°), the velocity triangle can be solved, showing that the forearc at 14°N moves at 27 mm/yr relative to the forearc south of 10°N.

Aleutians

Along the Aleutian arc, there are few earthquake slip vectors west of 175°E (Figure 1b) that can be used to constrain the deformation of the forearc. Nevertheless, we can make a prediction about the arc-parallel strain rate there with (7). Using $\Psi_{\max}=35^\circ\pm 10^\circ$, $d\gamma/dx=0.0367\pm 0.0022$ deg/km (change in obliquity of 68° along 1850 km of trench from 164°E to 189°E), and v varying from 78 mm/yr at 164°E to 72 mm/yr at 189°E, we get arc-parallel strain rates of 5 to 7 $\times 10^{-8}$ /yr near 181°E and 3 to 6 $\times 10^{-8}$ /yr near 165°E. Ekström and Engdahl [1989] suggested that the slip rate of the Aleutian forearc relative to the North American plate increased from 0 to 50 ± 10 mm/yr between 170°E and 200°E (a distance along the trench of 2200 km) for an average strain rate of $2.3\pm 0.5 \times 10^{-8}$ /yr. Geist et al. [1988] estimated the total strain

in the forearc between 172°E and 188°E over the past 5 to 6 Ma at 9% to 10% for a strain rate of 1.5 to 2.0×10^{-8} /yr; this geologic estimate agrees better with the *Ekström and Engdahl* [1989] strain rate than with mine, assuming that the present rate is the same as the average rate since 5 Ma.

The discrepancy is probably due to the result of applying the simple model that Ψ_{\max} is constant along the arc; this result derives from the assumptions on the mechanical behavior of the blocks and their boundaries. The slip vectors from the Aleutian arc provide an important clue as to the appropriate rheological properties to use. We can think of the apparent increase in Ψ with increasing obliquity (for $\gamma > 35^\circ$; Figure 6d) as an increase in R_f which, as viewed through the simple model, means that the force on (or strength of) the upper plate increases relative to that on the thrust plane. If the geometry along strike remains the same with the exception of the obliquity, then the yield stress of the upper plate increases with the strain rate, because strain rate depends on the angle γ - Ψ (Figure 3). Therefore I suggest that the Aleutian forearc would probably be represented better with an elastic-plastic (with strain hardening) rheology than by the elastic-perfectly plastic rheology that I have used in my derivation. Although these suggestions are preliminary and rely on a number of untested assumptions, clearly the next step is to use the slip vector data to constrain the mechanical properties of forearcs.

DISCUSSION

The analysis presented above for all its simplicity can explain why earthquake slip vectors at oblique subduction zones fall between the trench-normal and the plate convergence directions. The analytical result provides insight into the physical parameters that may control the partitioning of slip in oblique convergence although, as we have seen for the Sumatra example, because of the great uncertainties in the dimensions of the faults, in most cases it is unlikely that one can place useful constraints on the values of the stress ratios in the real world by making observations of slip vector deflections.

Nevertheless, the conclusion that forearcs of subduction zones at which the angle of obliquity changes along strike will stretch or shrink along strike is supported by observation and has important implications for the geologic evolution of convergent margins. Arc-parallel gradients in oblique convergence occur at many subduction zones (Figure 4), and tectonic maps showing relative plate vectors reveal many examples of variations of the convergence angles in the manner of Figure 5. Many forearcs may be deforming at present. Geologic and seismologic evidence has been presented for modern extension of the Aleutian arc [*Geist et al.*, 1988; *Ekström and Engdahl*, 1989; *LaForge and Engdahl*, 1979]. *Huchon and LePichon* [1984] and *Harjono et al.* [1991] suggest that the Sunda Strait just southwest of Sumatra has opened by arc-parallel extension, and it is clear that arc-parallel extension occurs in the Andaman Sea north of Sumatra [*Curray et al.*, 1979]. In the southern Banda arc, where the Timor trough bends to the northeast and plate convergence becomes oblique, two shallow earthquakes (<10 km depth and body-wave magnitudes of 5.6 and 5.8) with normal-faulting mechanisms striking perpendicular to the trench occurred beneath the forearc at the north coast of Timor island [*McCaffrey*, 1988]. Modern arc-parallel extension of the forearc has also been suggested for the southwestern Kuril arc [*Kimura*, 1986] and the southwest Ryukyu arc [*Kuramoto and Konishi*, 1989]. Oblique convergence between India and Eurasia may also contribute to extension in Tibet.

The analysis presented here does not assume or provide insight into how the forearc deforms because the slip vectors are insensitive to the details of the deformation [*McCaffrey*, 1991]. The Aleutian arc appears to deform mainly by the rotation and translation of large blocks of the forearc [*Geist et al.*, 1988]. The rotations of the blocks will locally deflect the slip vectors, but the average of the slip vector azimuths over the length of the block will reflect the component of translation. Rotations of blocks about vertical axes may be a significant source of the large scatter in slip vectors (Figure 1).

Oblique convergence may in some cases drive deformation in the backarc region, but such deformation cannot alone account for the strain needed to accommodate oblique convergence. Because the forces that drive slip partitioning in oblique convergence act across the thrust fault beneath the forearc, the forearc must respond in some way to these forces. If the forces are also to act on the strike-slip fault and backarc regions, then the forearc has to deform in some manner (what we often call "transmission of stress" is in fact accomplished by strain). The strain of the forearc in response to the forces may be elastic, in which case the slip vectors are not deflected from the plate convergence direction, or anelastic, which will deflect the slip vectors. The important point is that even though backarc deformation may be an obvious manifestation of oblique convergence, we should still look to the forearc for evidence of deformation that may be an important part of the story. As a rule, once the backarc deformation is understood, one should ask whether or not the forearc can behave as a rigid plate in the particular tectonic setting while matching the orientations of the slip vectors at the trench. In my view, only rarely will the answer to this be yes.

It is likely that many convergent margins in the past have undergone a spatial variation in the convergence angle and were deformed in response. If the geometry was such that the margin was stretching, one might expect to see normal faults striking roughly across the forearc, although the arc-parallel extension could be accommodated in other ways. Besides the Aleutians and Sumatra, margin-perpendicular normal faults have also been described in the Ryukyu arc [*Kuramoto and Konishi*, 1989] and in the Cretaceous plate margin of Venezuela [*Avé Lallement and Guth*, 1990]. Strain indicators in blueschist and eclogite bearing terranes probably from accretionary wedges and forearcs suggest that extension has occurred parallel to plate margins in Japan [*Toriumi and Noda*, 1986], Washington [*Brown and Talbot*, 1989], and Venezuela [*Avé Lallement and Guth*, 1990].

Arc-normal extension has been suggested to be an important mechanism to bring high-pressure, low-temperature metamorphic rocks to shallow levels in accretionary wedges [e.g., *Platt*, 1986]. The arc-parallel strain rates estimated here for the Sumatran, Aleutian, and Philippine forearcs indicate that forearcs could thin at a rate of 1 to 2 mm/yr by arc-parallel extension (assuming a 40 km thick incompressible forearc that deforms only by thinning in the vertical and extending in the arc-parallel direction). Because a forearc wedge probably thickens by accretion of material to its toe or to its base [e.g., *Moore and Silver*, 1987], it is likely that this rate of thinning is also the rate at which deeper rocks approach the upper surface of the accretionary wedge and represents a significant contribution to the exhumation rate of the metamorphic rocks.

CONCLUSIONS

In oblique subduction zones, slip vectors often point between the direction of plate convergence and the normal to the trench, with a preference, at least in Sumatra, the Aleutians, and the Philippine trench, to follow the trench-normal rather than the orientation of relative plate motion. I have shown that this behavior is predicted by a model of oblique convergence that can be derived from force equilibrium conditions. If obliquity becomes large, the angle that the slip vector makes with the normal to the trench will reach a constant value that depends, in this simple model, on the ratio of the shear forces on the transcurrent and subduction faults. This angle is recoverable from the variation in slip vectors of earthquakes, but its usefulness to constrain the ratio of stresses is limited in the real world because of the uncertainties in the vertical extents of the faults and because obliquity varies significantly along strike of most modern trenches. An important geological implication of this analysis is that if obliquity varies along a subduction zone, then the forearc will stretch or shrink along strike, depending on whether it is convex or concave toward the subducting plate side. The analysis here provides a way to estimate the rate of deformation of the forearc in such cases. The forearc at Sumatra stretches along strike with a uniform strain rate of about 1 to 3×10^{-8} /yr; this implies an increase in the slip of the

forearc relative to Southeast Asia of up to 60 mm/yr along the margin. The Aleutian forearc stretches at a rate of 2 to 6×10^{-8} /yr and the Philippine forearc stretches at about 0.3 to 3×10^{-8} /yr. Arc-parallel extension may be more common than generally appreciated and may be an important mechanism to bring high-grade metamorphic rocks to shallow levels in accretionary wedges.

Acknowledgments. Thanks to Peter Molnar for convincing me to balance forces rather than minimizing work and his help in the derivation, to Steve Roecker, Frank Spear, John Platt, Brian Bayly, Kerry Sieh, and Craig Jones for discussions, to Myrl Beck, Richard Gordon, and Andy Michael for helpful reviews, to Hans Avé Lallemant for providing references on stretching forearcs, and to Mary Carey for preparation of the manuscript. Supported by NSF Grants EAR-8903762 and EAR-8908759.

REFERENCES

- Abers, G.A., and R. McCaffrey, Active deformation in the New Guinea fold-and-thrust belt: seismological evidence for strike-slip faulting and basement-involved thrusting, *J. Geophys. Res.*, **93**, 13,332-13,354, 1988.
- Avé Lallemant, H.G., and L.R. Guth, Role of extensional tectonics in exhumation of eclogites and blueschists in an oblique subduction setting, northwest Venezuela, *Geology*, **18**, 950-953, 1990.
- Barrier, E., P. Huchon, and M. Aurelio, Philippine Fault: A key for Philippine kinematics, *Geology*, **19**, 32-35, 1991.
- Beck, M., On the mechanism of tectonic transport in zones of oblique subduction, *Tectonophysics*, **93**, 1-11, 1983.
- Beck, M., Model for late Mesozoic-early Tertiary tectonics of coastal California and western Mexico and speculations on the origin of the San Andreas fault, *Tectonics*, **5**, 49-64, 1986.
- Beck, M., Coastwise transport reconsidered: lateral displacements in oblique subduction zones, and tectonic consequences, *Phys. Earth Planet. Int.*, **68**, 1-8, 1991.
- Bird, P., and D.A. Yuen, The use of a minimum-dissipation principle in tectonophysics, *Earth Planet. Sci. Lett.*, **45**, 214-217, 1979.
- Brown, E.H., and J.L. Talbot, Orogen-parallel extension in the North Cascades crystalline core, Washington, *Tectonics*, **8**, 1105-1114, 1989.
- Curray, J.R., D.G. Moore, L.A. Lawver, F.J. Emmel, R.W. Raitt, M. Henry, and R. Kieckhefer, Tectonics of the Andaman Sea and Burma, in *Geological and Geophysical Investigations of Continental Slopes and Rises*, *AAPG Mem.*, **29**, 189-198, 1979.
- DeMets, C., R.G. Gordon, D.F. Argus, and S. Stein, Current plate motions, *Geophys. J. Int.*, **101**, 425-478, 1990.
- Dziewonski, A.M., T.-A. Chou, and J.H. Woodhouse, Determination of earthquake source parameters from waveform data for studies of global and regional seismicity, *J. Geophys. Res.*, **86**, 2825-2852, 1981.
- Ekström, G. and E.R. Engdahl, Earthquake source parameters and stress distribution in the Adak Island region of the central Aleutian Islands, Alaska, *J. Geophys. Res.*, **94**, 15,499-15,519, 1989.
- Fitch, T.J., Plate convergence, transcurrent faults and internal deformation adjacent to southeast Asia and the western Pacific, *J. Geophys. Res.*, **77**, 4432-4460, 1972.
- Geist, E.L., J.R. Childs, and D.W. Scholl, The origin of summit basins of the Aleutian Ridge: Implications for block rotation of an arc massif, *Tectonics*, **7**, 327-341, 1988.
- Harjono, H., M. Diament, J. Dubois, and M. Larue, Seismicity of the Sunda Strait: Evidence for crustal extension and volcanological implications, *Tectonics*, **10**, 17-30, 1991.
- Huchon, P., and X. LePichon, Sunda Strait and central Sumatra fault, *Geology*, **12**, 668-672, 1984.
- Jarrard, R.D., Terrane motion by strike-slip faulting of forearc slivers, *Geology*, **14**, 780-783, 1986.
- Kanamori, H., Quantification of great earthquakes, *Tectonophysics*, **49**, 207-212, 1978.
- Kappel, E.S., Plate convergence in the Sunda and Banda arcs, B.A. Thesis, 40 pp., Cornell University, New York., 1980.
- Kimura, G., Oblique subduction and collision: Forearc tectonics of the Kuril arc, *Geology*, **14**, 404-407, 1986.
- Kuramoto, S., and K. Konishi, The southwest Ryukyu arc is a migrating microplate (forearc sliver), *Tectonophysics*, **163**, 75-91, 1989.
- LaForge, R., and E.R. Engdahl, Tectonic implications of seismicity in the Adak Canyon region, Central Aleutians, *Bull. Seismol. Soc. Am.*, **69**, 1515-1532, 1979.
- McCaffrey, R., Active tectonics of the eastern Sunda and Banda arcs, *J. Geophys. Res.*, **93**, 15,163-15,182, 1988.
- McCaffrey, R., Oblique plate convergence, slip vectors, and forearc deformation, *Eos Trans. AGU*, **71**, 1590, 1990.
- McCaffrey, R., Slip vectors and stretching of the Sumatran forearc, *Geology*, **19**, 881-884, 1991.
- McKenzie, D.P. and J. Jackson, The relationship between strain rates, crustal thickening, paleomagnetism, finite strain and fault movements within a deforming zone, *Earth Planet. Sci. Lett.*, **65**, 182-202, 1983.
- Michael, A.J., Energy constraints on kinematic models of oblique faulting: Loma Prieta versus Parkfield-Coalinga, *Geophys. Res. Lett.*, **17**, 1453-1456, 1990.
- Minster, J.B., and T.H. Jordan, Present-day plate motions, *J. Geophys. Res.*, **83**, 5331-5354, 1978.
- Molnar, P., Continental tectonics in the aftermath of plate tectonics, *Nature*, **335**, 131-137, 1988.
- Moore, J.C. and E.A. Silver, Continental margin tectonics: submarine accretionary prisms, *Rev. Geophys.*, **25**, 1305-1312, 1987.
- Mount, V.S., and J. Suppe, State of stress near the San Andreas fault: Implications for wrench tectonics, *Geology*, **15**, 1143-1146, 1987.
- Newcomb, K.R., and W.R. McCann, Seismic history and seismotectonics of the Sunda arc, *J. Geophys. Res.*, **92**, 421-439, 1987.
- Platt, J.P., Dynamics of orogenic wedges and the uplift of high-pressure metamorphic rocks, *Bull. Geol. Soc. Am.*, **97**, 1037-1053, 1986.
- Scholz, C.H., *The Mechanics of Earthquakes and Faulting*, 439 pp., Cambridge University Press, New York, 1990.
- Seno, T., T. Moriyama, S. Stein, D.F. Woods, C. Demets, D. Argus, and R. Gordon, Redetermination of the Philippine Sea plate motion, *Eos Trans. AGU*, **68**, 1474, 1987.
- Sieh, K., J. Rais, and Y. Bock, Neotectonic and paleoseismic studies in West and North Sumatra, *Eos Trans. AGU*, **72**, 460, 1991.
- Sykes, L., J.F. Pacheco, and C. Scholz, Nature of seismic coupling along simple plate boundaries of the subduction type, *Eos Trans. AGU*, **72**, 291, 1991.
- Toriumi, M., and H. Noda, The origin of strain patterns resulting from contemporaneous deformation and metamorphism in the Sumbagawa metamorphic belt, *J. Metamorph. Geol.*, **4**, 409-420, 1986.
- Walcott, R.I., Geodetic strains and large earthquakes in the axial tectonic belt of North Island, New Zealand, *J. Geophys. Res.*, **83**, 4419-4429, 1978.
- Zwick, P., and R. McCaffrey, Seismic slip rate and direction of the Great Sumatra Fault based on earthquake fault plane solutions, *Eos Trans. AGU*, **72**, 201, 1991.

R. McCaffrey, Department of Earth and Environmental Sciences, Rensselaer Polytechnic Institute, Troy, NY 12180-3590.

(Received May 18, 1991;
revised February 24, 1992;
accepted February 24, 1992.)